



Does an inter-flaw length control the accuracy of rupture forecasting in geological materials?



Jérémie Vasseur^{a,*}, Fabian B. Wadsworth^a, Michael J. Heap^b, Ian G. Main^c, Yan Lavallée^d, Donald B. Dingwell^a

^a Dept. of Earth and Environmental Sciences, Ludwig Maximilian University, Munich, Germany

^b Institut de Physique de Globe de Strasbourg (UMR 7516 CNRS), Strasbourg, France

^c School of Geosciences, University of Edinburgh, Edinburgh, UK

^d Dept. of Earth, Ocean and Ecological Sciences, University of Liverpool, Liverpool, UK

ARTICLE INFO

Article history:

Received 11 April 2017

Received in revised form 29 June 2017

Accepted 4 July 2017

Available online 27 July 2017

Editor: J. Brodholt

Keywords:

porous materials
inter-pore length
acoustic emission
precursors
rock failure
damage mechanics

ABSTRACT

Multi-scale failure of porous materials is an important phenomenon in nature and in material physics – from controlled laboratory tests to rockbursts, landslides, volcanic eruptions and earthquakes. A key unsolved research question is how to accurately forecast the time of system-sized catastrophic failure, based on observations of precursory events such as acoustic emissions (AE) in laboratory samples, or, on a larger scale, small earthquakes. Until now, the length scale associated with precursory events has not been well quantified, resulting in forecasting tools that are often unreliable. Here we test the hypothesis that the accuracy of the forecast failure time depends on the inter-flaw distance in the starting material. We use new experimental datasets for the deformation of porous materials to infer the critical crack length at failure from a static damage mechanics model. The style of acceleration of AE rate prior to failure, and the accuracy of forecast failure time, both depend on whether the cracks can span the inter-flaw length or not. A smooth inverse power-law acceleration of AE rate to failure, and an accurate forecast, occurs when the cracks are sufficiently long to bridge pore spaces. When this is not the case, the predicted failure time is much less accurate and failure is preceded by an exponential AE rate trend. Finally, we provide a quantitative and pragmatic correction for the systematic error in the forecast failure time, valid for structurally isotropic porous materials, which could be tested against larger-scale natural failure events, with suitable scaling for the relevant inter-flaw distances.

© 2017 Elsevier B.V. All rights reserved.

1. Introduction

All materials contain flaws with a large range of length scales, from kilometre-sized fractures in the crust (Hatton et al., 1994), to meter-sized cavities (Castro et al., 2002) and fractures in rocks and synthetic materials (Allègre et al., 1982), down to micro- and nano-pores and density fluctuations in thin-film glasses (Guyer and Dauskardt, 2004) and crystals. These flawed materials eventually rupture in catastrophic failure events when applied stresses become sufficiently large to produce system-spanning fractures (Sammis and Ashby, 1986). Recent efforts have converged and found that two observations dominate the physics of failure of these systems. First, the flaws in the system concentrate stress relative to the unflawed domains of the material and therefore

the flaw fraction in the material exerts a first-order control on the far-field stress required for macroscopic failure (Kemeny and Cook, 1986; Sammis and Ashby, 1986; Vasseur et al., 2013). Second, the size of flaws and the inter-flaw length determine the extent to which the cracks that emanate from flaws will interfere (Bažant, 2004; Sornette and Andersen, 1998). These two paradigms underpin all elastic models of rupture events in heterogeneous solids and predict that, as the material approaches macroscopic failure, the rate of energy released as acoustic emissions (AEs) by microscopic failure events accelerates (Kilburn, 2012; Lockner et al., 1991; Scholz, 1968; Turcotte and Newman, 2003; Vasseur et al., 2015; Voight, 1989). When first proposed, the finding that these bulk-material accelerations in the rate of energy release or event number approaches a singularity that coincided with the failure time provided a tantalizing possibility that material failure could be forecast accurately using indirect observations such as micro-earthquakes or AEs prior to wholesale rupture

* Corresponding author.

E-mail address: jeremie.vasseur@min.uni-muenchen.de (J. Vasseur).

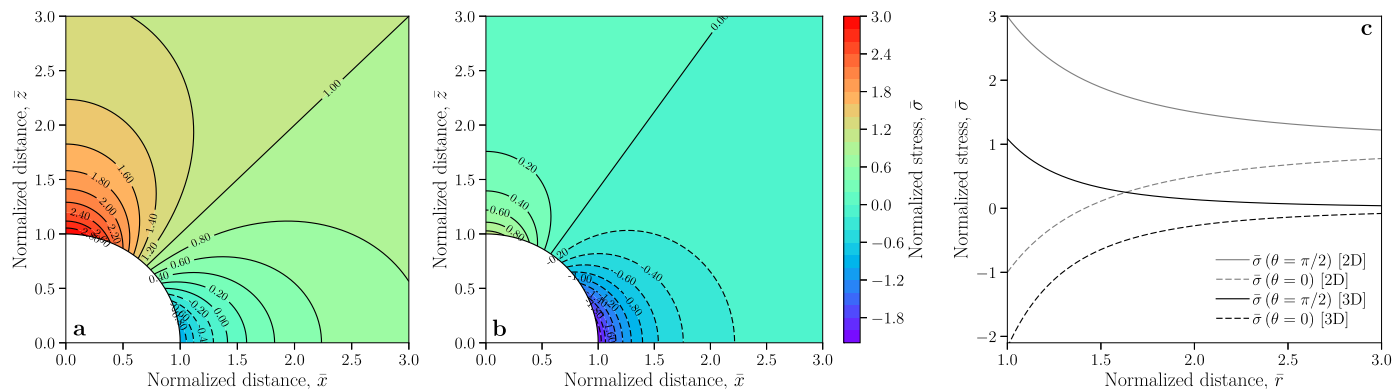


Fig. 1. Stress around pores in 2D and 3D. The distances are normalized by the cavity radius a and the stress by the far-field applied stress σ_1 . (a) The total stress distribution around a circular pore in an infinite plate (2D) mapped out in the positive quadrant of the x - z plane as calculated by combining Eqs. (S1)–(S3). (b) The total stress distribution around a spherical pore in an infinite body (3D) mapped out in the positive quadrant of x - z plane as calculated by combining Eqs. (S4)–(S7). (c) The total stress resolved along the z -axis ($\theta = \pi/2$) and along the x -axis (2D) or the x - y plane (3D) ($\theta = 0$).

(Voight, 1989). Indeed a large effort has been expended in assessing the utility of this tool for forecasting hazardous failure phenomena in nature (Bell et al., 2011; Bell and Kilburn, 2013; Hao et al., 2016; Kilburn et al., 2017; Robertson and Kilburn, 2016; Voight, 1988). However, the still-limited success of these methods (Bell et al., 2013) has highlighted complexities in the approach to failure of heterogeneous materials that must be addressed if forecasting tools are going to be of the widest utility.

2. Micromechanical models for the uniaxial deformation of porous materials

Here we present a linear elastic model to demonstrate quantitatively how stress is distributed around a circular (2D) or spherical (3D) cavity in an infinite solid and exposed to a far-field stress. Then we follow previous work to scale that concept to a porous body with finite dimensions in order to predict the failure stress of a porous material as a function of the porosity ϕ and the pore radius a . We focus on the uniaxial case in which far-field stresses are applied in one direction only, and later we discuss how our findings could be extended to more complex stress configurations in principle. Finally, we explore other characteristic length scales in natural materials that may be more relevant than the pore size; namely, the inter-pore and inter-particle distances.

2.1. The concentration of uniaxial applied stress around circular and spherical pores

First we use a linear elastic model for the stress distribution around a circular (2D) or spherical (3D) cavity. For the 2D case we opt for the solution credited to Kirsch (1898) and to Goodier (1933) for the 3D case, repeated in variable completeness in subsequent work (Jaeger et al., 2009; Soutas-Little, 1999) with which the stress components can be computed for each spatial position around a cavity of radius a . We use the Cartesian coordinate system with the far-field stress applied in the z -direction and the centre of the pore positioned at $(x, y, z) = 0$. A line of length r away from the pore centre in any direction subtends an angle with the z -axis of θ and an angle with the x - or y -axes of ψ . In what follows, we normalize each axis (x, y, z) and the radial direction r by a and the individual stress components τ_{ij} by the far-field applied stress σ_1 , yielding a coordinate system and stress tensor components for which a bar above the parameter denotes its normalized value. We introduce the 2D and 3D stress components in the supplementary file as Eqs. (S1)–(S3) and Eqs. (S4)–(S7).

In Fig. 1, we present the normalized stress as a colour map around a 2D circular cavity (Fig. 1a) and a 3D spherical cavity using $\nu = 0.25$ (Fig. 1b), which is a first-order approximation for crustal rocks (assuming the two Lamé parameters are equal). The lobes of concentrated stress are compressive in the region of the solid surrounding the z -axis and are tensile in the region of the solid about the x -axis (2D) or the x - y plane (3D). It is in these lobes of concentrated stress that fractures would be most likely to initiate. For this reason, in Fig. 1c we additionally show the stress resolved along the z -axis ($\theta = \pi/2$) and along the x -axis (2D) or the x - y plane (3D) ($\theta = 0$).

2.2. Approximate methods for predicting the stress required for rupture

The deformation of elastic porous media results in cracks that propagate from interfaces at which stress is locally concentrated relative to the far-field applied load (Sammis and Ashby, 1986). Sammis and Ashby (1986) present a static so-called *pore-crack* model to compute the degree to which stress is concentrated around cavities (a cavity stress intensity factor K_{ji}) and the degree to which cracks that grow from those cavities interact (a crack interaction stress intensity factor K_{jii}). Their solutions are cast as simple functions of the sample porosity ϕ , rendering them easy to use and to compare with measured data (Zhu et al., 2011). Where the *pore-crack* model is used, only the solution for 2D is usually compared with experimental data (Baud et al., 2014; Zhu et al., 2011). Here we apply the *pore-crack* model (Sammis and Ashby, 1986) in uniaxial conditions where the sum of K_{ji} and K_{jii} is the total stress intensity K_I .

When a far-field stress σ_1 is applied ($\sigma_2 = \sigma_3 = 0$) onto a material rupture begins only when the local stress σ exceeds σ_c . At this point a fracture can initiate to a distance c away from the pore or cavity at which distance $\sigma = \sigma_c$, and beyond which $\sigma < \sigma_c$. This distance c is the equilibrium crack length for the stress state at a given time and, defined in non-dimensional form as $\bar{c} = c/a$. Then \bar{c} as a function of a normalized stress $\bar{\sigma} = \sigma\sqrt{\pi a}/K_{Ic}$ (where K_{Ic} is the fracture toughness or critical stress intensity required for crack propagation in the solid) for the 3D and uniaxial case, is as follows (Sammis and Ashby, 1986)

$$\bar{\sigma} = \left(\frac{0.62\sqrt{\bar{c}}}{(1+\bar{c})^{4.1}} + \frac{\sqrt{2\phi(1+\bar{c})}}{\pi} \right)^{-1} \quad (1)$$

where the first term on the right-hand side of Eq. (1) describes the growth of a crack from a single pore, while the second term is a crack-interaction term related to the porosity ϕ (see Sammis and Ashby, 1986 for full description). This model neglects time-dependency and therefore it is implicitly assumed that the cracks

Download English Version:

<https://daneshyari.com/en/article/5779667>

Download Persian Version:

<https://daneshyari.com/article/5779667>

[Daneshyari.com](https://daneshyari.com)